An Investigation of Moisture Gradient in Wood during Drying Using X-Ray Radiation and Numeric Methods

Le Yu Xiaofeng Hao Liping Cai Sheldon Q. Shi
Jiali Jiang Jianxiong Lu

Abstract

The moisture gradient in wood is a characteristic of major interest in lumber drying. Two methods, an ovendry slicing method and an X-ray scanning method, were used to examine moisture gradients in wood during the drying of Chinese fir (*Cunninghamia lanceolata*). The results of the comparison between these two methods confirmed that X-ray radiation can be used to monitor moisture distribution during the drying of Chinese fir. Compared with the moisture content (MC) values obtained by the ovendry slicing method, the X-ray scanning method is capable of determining MC to within ±12.9 percent. Using a control volume approach, a numeric model for estimating the moisture gradient in wood during drying was developed in this work. The validation tests indicated that the model can be used to estimate moisture gradients during the drying of Chinese fir and is capable of predicting moisture distribution to within ±12.6 percent.

The moisture gradient in wood is one of the most important physical parameters that needs to be accurately examined if the goal is to obtain high-quality dried lumber in terms of minimized internal stresses and good dimensional stability. Many efforts have been made to precisely measure the moisture content (MC) gradient in wood. To determine moisture diffusion coefficients using an inverse algorithm, moisture gradients during drying have been measured by slicing thin layers with a band saw (Liu et al. 2001) or a microtone knife (Cai 2005b). Although acceptable results were obtained, these specimens were destroyed after measuring MC, and thus these methods failed to provide continuous monitoring of the moisture movement inside the wood. This made it difficult to develop accurate models of the moisture gradient and movement during wood drying.

Wood density is another characteristic of major interest that can be used as an indicator of the strength and quality of wood. Using a medical computed axial tomographic scanner, X-ray absorption coefficients and computer tomographic (CT) numbers, as well as their relation to wood density, were investigated (Lindgren 1991). It was found that dry wood density could be measured to an accuracy of ±4 kg/m^3. Since wood with the same density but different contents of water had different X-ray absorption coefficients, moist wood density could be measured to an accuracy of ±13.4 kg/m^3. The effect of the width of the annual growth rings on density has also been explored (Lindgren et al. 1992). The results demonstrated that the density could be reliably determined using an X-ray microscanner when the annual growth rings were about 0.9 mm or greater in width. After applying a calibration procedure, X-ray computer tomography was used to rapidly estimate wood density (Freyburger et al. 2009). It was concluded that the calibration method enabled the use of a medical scanner to obtain accurate wood density in a fast and nondestructive way.

The authors are, respectively, Master's Student, College of Material Sci. and Engineering, Central South Univ. of Forestry and Technol. of China, Changsha, People's Republic of China (yule731226@163.com); PhD Candidate, Key Lab. of Wood Sci. and Technol. of State Forestry Admin., Research Inst. of Wood Industry, Chinese Academy of Forestry, Beijing, People's Republic of China (hxf8271@163.com); Research Scientist and Associate Professor, Mechanical and Energy Engineering Dept., Univ. of North Texas, Denton (Liping.Cai@unt.edu, sheldon.shi@unt.edu); Associate Professor, Key Lab. of Wood Sci. and Technol. of State Forestry Admin., Research Inst. of Wood Industry, Chinese Academy of Forestry, Beijing, People's Republic of China (jialiwood@caf.ac.cn); and Professor, College of Material Sci. and Engineering, Central South Univ. of Forestry and Technol. of China, Changsha, and Key Lab. of Wood Sci. and Technol. of State Forestry Admin., Research Inst. of Wood Industry, Chinese Academy of Forestry, Beijing, People's Republic of China (jianxiong@caf.ac.cn [corresponding author]). This paper was received for publication in January 2014. Article no. 14-00007.

Forest Prod. J. 64(5/6):199–205.
doi:10.13073/FPJ-D-14-00007

Using a medical X-ray CT scanner, a regression model for precisely estimating the average M was developed based on the information from tests of small specimens (2 by 2 by 1 cm) by Hattori and Kanagawa (1985). After establishing the model, Kanagawa and Hattori (1985) examined moisture distributions of two 10.5-cm^2 timbers during conventional kiln drying. It was found that the average M during drying could be estimated using CT images and the regression model. Using a CT scanner, Pang and Wiberg (1998) examined moisture distribution within *Pinus radiata* sapwood boards during drying when the wood's basic density profile was known. Using an industrial CT, Alkan et al. (2007) examined subalpine fir lumber with wet pockets. The results showed that the drying development pattern at each increment from core to shell was much slower in the wet-pocket zones than in the normal wood regions along the width, thickness, and length of the board.

However, CT scanning is slow, complex, and expensive due to its multiorientation shooting (Baettig et al. 2006). X-ray absorptiometry is simpler and more accessible for determining MC in wood. Baettig et al. (2006) successfully measured MC profiles in a Norway spruce (*Picea abies*) board during vacuum drying by placing an X-ray source and an energy-sensitive detector on both sides of a laboratory vacuum kiln. Cai (2008) employed a collimated radiation beam (X-rays or gamma rays) emitted from a radiation source. A radiation detector recorded the intensities of the transmitted beams. The MC gradients were calculated by contrasting them to the ovendried density profiles. After comparing the radiation results with the measured MC gradients using the ovendry method, it was confirmed that the radiation method could provide an accurate and prompt estimation of internal wood MC gradient. Watanabea et al. (2008) used a digital X-ray microscope to measure MC of Japanese cedar (*Cryptomeria japonica*) and evaluated its accuracy compared with the values that were determined using the typical ovendry method. It was found that the standard error achieved was about 1 percent MC within the experimental range.

The wood-drying model is a powerful tool for understanding and quantifying moisture movement in wood during drying and can be used to improve productivity and dried-wood quality (Pang 2007). Pang and Wiberg (1998) used the CT-scanned results to validate a two-dimensional single-board drying model. The validation indicated that the model was capable of predicting the MC gradients in board thickness and width and within growth rings. Haquea (2007) developed a two-dimensional drying model to simulate MC profiles during high-temperature drying for industrial drying schedules. It was found that the effects of specific heat capacity and thermal conductivity on the overall drying rate of the board were insignificant. However, the effect of changes in the diffusion coefficient on the drying rate below the fiber saturation point was significant. Cai and Oliveira (2008) simulated the performance of moisture distribution during the drying of wet-pocket lumber. Zhang and Cai (2011) estimated moisture gradients during high-temperature drying of subalpine fir (*Abies lasiocarpa*) through microscopic analysis.

This study was aimed at investigating the development of moisture gradients in Chinese fir wood during drying using three approaches, namely, X-ray radiation, the numeric method, and the traditional ovendrying method.

Materials and Methods

Sample preparation and drying process

Sourced from Hunan Province, China, a Chinese fir (*Cunninghamia lanceolata*) log with a diameter of 36 cm was shipped to the laboratory in Beijing, China. As shown in Figure 1, blocks 185 mm wide, 45 mm thick, and 1,000 mm long were flat sawn from the log, and each block was split into two specimens with dimensions 90 by 45 by 1,000 mm.

One specimen was used for the determination of the MC gradient using X-ray radiation, and another was used for the determination of the MC gradient using ovendried sliced samples. The MC was approximately 50 percent. Prior to drying, each specimen was painted on all edges with two coats of heavy epoxy to restrict moisture movement to a thickness of 45 mm (radial direction).

A laboratory-made dryer with an accuracy of ±1°C was used and all experiments used a preset air velocity of 1.5 m/s. The dryer was heated from room temperature to the dry-bulb/wet-bulb temperatures of 75°C/63°C (about 58% relative humidity) in 1 hour and remained constant for the whole drying process. The specimens were periodically (6, 30, 45, 70, 100 and 120 h) taken out from the dryer. At each drying period, after an approximately 10-mm end was trimmed, three samples measuring 45 by 45 by 45 mm were cut from each specimen using a small band saw (Fig. 1). The precise dimensions of each sample were measured using a caliper. After the samples were cut, the end of each specimen was sealed by epoxy before it was placed back in the dryer. During the slicing process, each sample was sliced into 21 sections using a laboratory-made cutting tool. Therefore, each gradient section was approximately 2.14

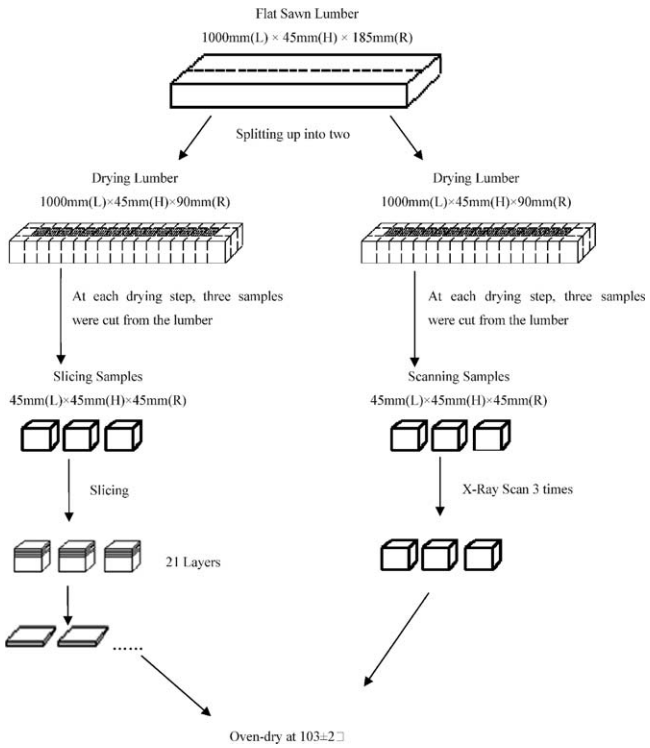

Figure 1.—Sample preparation and drying process.

mm in thickness. Immediately after being sliced, each section was weighed and oven-dried to determine its MC.

X-ray examination

The X-ray radiation system DENSE-LAB X was used in this study. The X-ray source and the detector were placed together on two motorized stages with an accurate positioning control, which were then set in a rigid framework. When an X-ray beam penetrated a specimen (Fig. 2), the ratio of intensity I to incident intensity I_0 could be given by the exponential attenuation law,

$$\frac{I}{I_0} = e^{-\mu\rho t} \tag{1}$$

where I and I_0 are intensity and incident intensity, μ is the mass attenuation coefficient (cm^2/g), ρ is the raw density of wood (kg/m^3), and t is the transmitted distance in wood (cm). When the I_0/I, μ, and t are known, the wood's average density in the X-ray–penetrated zone can be obtained:

$$\rho = \frac{1}{\mu t}\ln\left(\frac{I_0}{I}\right) \tag{2}$$

In order to examine moisture distribution in the thickness direction during drying, the X-ray–scanned sample was also sliced into 21 sections. The average density was obtained using linear interpolation approximation and the weighted average method. Based on the density, dimension, ovendried density, and ovendried dimensions of the section, the average MC of the section could be calculated as follows:

$$\begin{aligned} MC_{i,j} &= \frac{w_{i,j} - w_{0,j}}{w_{0,j}} \times 100\% \\ &= \frac{\rho_{i,j}L_{i,j}T_{i,j}h_{i,j} - \rho_{0,j}L_{0,j}T_{0,j}h_{0,j}}{\rho_{0,j}L_{0,j}T_{0,j}h_{0,j}} \times 100\% \end{aligned} \tag{3}$$

where MC is the moisture content (%), W is the weight of the section (g), ρ is the raw density of wood (kg/m^3), L is the length of the section (mm), T is the width of the section (mm), and h is the thickness of the section (mm). Subscript i is the ith drying period ($i = 1, 2, \ldots 7$), o is the final ovendrying period, and j is the jth section ($j = 1, 2, \ldots 21$).

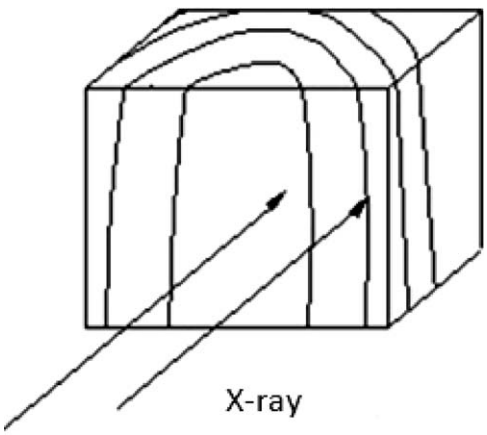

Figure 2.—X-ray beam penetrated the specimen.

Development of the numeric model

Consider the specimen with thickness $2h$ as shown in Figure 3. When moisture moves in the direction of the thickness (h) of the specimen, a one-dimensional model can be used (Cai 2005a). When the density, thermal conductivity, and specific heat of the lumber are known, the governing equation for the conservation of energy is as follows:

$$\rho C_p \frac{\partial T}{\partial t} = \frac{\partial}{\partial x}\left(k\frac{\partial T}{\partial x}\right) \quad \text{for } 0 < x < h,\ t > 0 \tag{4}$$

where T is the temperature (°C), k is the thermal conductivity (W/m·K), ρ is the basic density of wood (kg/m^3), C_p is the specific heat of wood (J/kg·K), t is the time (s), and x is the space coordinate. The boundary conditions were shown in the following forms:

$$-k\frac{\partial T}{\partial x} = h_h(T_s - T_\infty) \quad \text{at } x = 0 \tag{5}$$

where T_s is the surface temperature (°C), T_∞ is the temperature in the kiln (°C), and h_h is the heat transfer coefficient ($W/m^2\cdot K$). Because a relatively low air velocity was used in this case, a value of $h_h = 2.4$ $W/m^2\cdot K$ was used (Pordage and Langrish 1999):

$$\frac{\partial T}{\partial x} = 0 \quad \text{at } x = h \tag{6}$$

and the initial condition can be written as follows:

$$T(x, 0) = T_{\text{initial}} \tag{7}$$

The governing equation for the conservation of mass is as follows:

$$\frac{\partial C}{\partial t} = \frac{\partial}{\partial x}\left(D\frac{\partial C}{\partial x}\right) \quad 0 < x < h,\ t > 0 \tag{8}$$

where C is the moisture concentration (kg/m^3), t is time (h), D is the diffusion coefficient (mm^2/h), and x is the space coordinate measured from the center of the specimen. The initial condition was

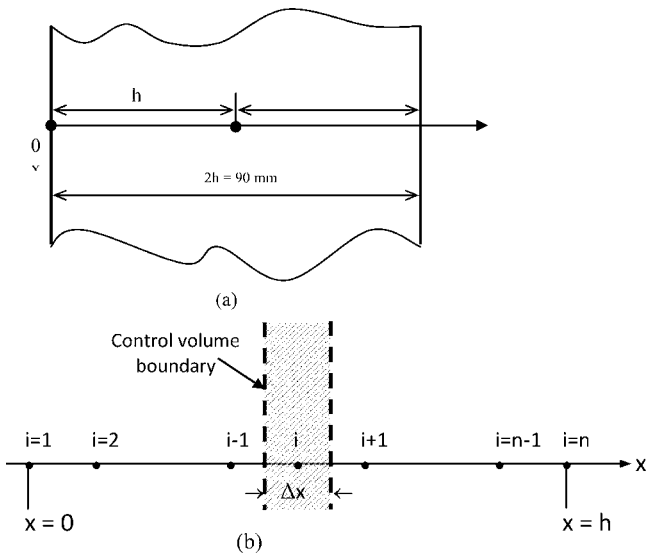

Figure 3.—(a) Test specimen; (b) discretization of space coordinate.

$$C = C_0;\ C < h,\ t = 0 \tag{9}$$

where C_0 is the initial moisture concentration (kg/m^3).

Half of the specimen thickness (h) was discretized with mesh width (Δx) in space (Fig. 3b). The boundary condition at the center of the specimen was

$$\frac{\partial C}{\partial x} = 0 \quad x = h,\ t \geq 0 \tag{10}$$

and the boundary condition at the surface of the specimen was

$$-D\frac{\partial C}{\partial x} = h_m(C_s - C_\infty) \quad x = 0, t>0 \tag{11}$$

where C_s is the moisture concentration on the surface of wood (kg/m^3), C_∞ is the moisture concentration of the air (kg/m^3), and h_m is the mass transfer coefficient (m/s), which may be expressed as

$$h_m = \frac{h_h}{\rho_g C_{pg}}\left(\frac{P_r}{S_c}\right)^{\frac{2}{3}} \tag{12}$$

where h_h is the heat transfer coefficient (W/m^2·K), ρ_g is the density of air (kg/m^3), C_{pg} is the specific heat capacity (J/kg·K), P_r is Prandtl number, and S_c is the Schmidt number.

The coupled partial-differential Equations 4 and 8 were solved using the control volume method (Kreith and Bohn 2001). A control volume is a fixed region in space bounded by a control surface through which heat and mass pass. The first law of thermodynamics states that energy can be neither created nor destroyed but can be transformed from one form to another. In the control volume, the rate at which heat and moisture enter plus the rate at which heat is generated within that volume minus the rate at which heat and moisture leave the volume must equal the rate at which heat and mass are stored inside this volume. Using this method, the heat and mass transfer process during wet-pocket lumber drying was successfully simulated (Cai and Oliveira 2008).

As shown in Figure 3b, half of the specimen thickness (h) was discretized with the width (Δx) in space. To consider a mass balance on this control volume, the rate at which mass moves into the control volume equals the rate at which mass moves out of the control volume. Then

$$\begin{aligned} -D\frac{dC}{dx}(\text{in}) &= -D\frac{C_{i+1} - C_i}{\Delta x} = -D\frac{dC}{dx}(\text{out}) \\ &= -D\frac{C_{i-1} - C_i}{\Delta x} \end{aligned} \tag{13}$$

For an unsteady mass transfer problem, a discrete time step Δt was introduced:

$$t_m = m\Delta t \quad m = 0, 1, 2, \ldots \tag{14}$$

The equations were rearranged as:

$$C_{i,m+1} = C_{i,m} + \frac{\Delta t}{\Delta x^2} D(C_{i+1,m} - 2C_{i,m} + C_{i-1,m}) \tag{15}$$

Because the diffusion coefficients of Chinese fir in a similar environment are not available, the data from western red cedar (*Thuja plicata*) determined by Koumoutsakos and Avramidis (2002) were used. When the drying temperature was 70°C and the average MC was about 5 percent, the average diffusion coefficient in the radial direction was approximately $(1.47 + 0.96)/2 = 1.22 \times 10^{-10}$ m^2/s.

Results and Discussion

During the drying process, the MC values obtained by ovendrying sliced sections, X-ray scanning, or model calculating were averaged at each time period. A comparison among the ovendry-determined (SlicingM) and X-ray–determined (X-rayM) MC values and the calculated curve (CalcM) using the model is presented in Figure 4. As shown, the differences among the average MC values were minor, and the calculated curve exactly follows the X-ray–scanned and ovendry-determined values.

Figures 5 through 11 present the comparison of MC gradients among the SlicingM values, X-rayM values, and CalcM using the model. As shown in these figures, the differences of MC between the ovendry slicing method and X-ray–determined values were slight. It was suggested that X-ray radiation can be used for monitoring moisture movement and distribution during drying to provide prompt information about internal stresses that could result in warping and defect development.

Table 1 illustrates a comparison of MC at several characteristic layers in the samples among the three

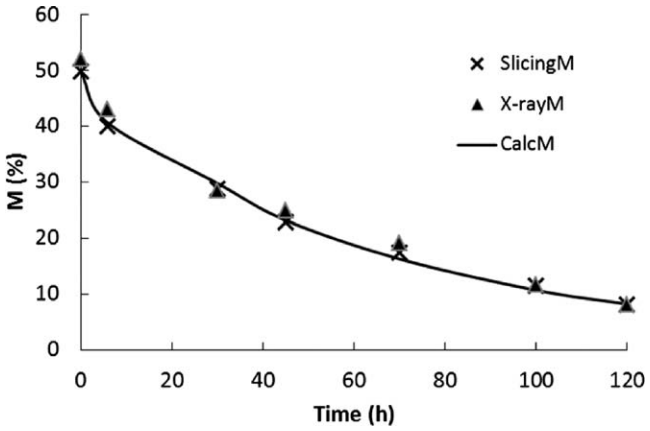

Figure 4.—A comparison among the ovendry-determined (SlicingM) and X-ray–determined (X-rayM) values, and calculated curve (CalcM) using the model.

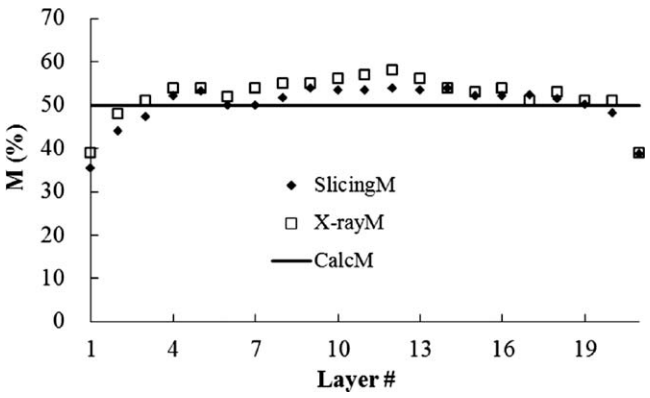

Figure 5.—Initial moisture content gradients. SlicingM = ovendry-determined values; X-rayM = X-ray–determined values; CalcM = calculated curve.

Table 1.—A comparison of moisture content gradients among the three methods.[a]

Drying period (h)		Layer: 1	4	7	10	13	16	19	21	Avg.
0	SlicingM	35.1	52.0	49.8	53.2	53.2	52.0	50.0	38.4	
	X-rayM	39.0	54.0	54.0	56.0	56.0	54.0	51.0	39.0	
	Abs. Dev. 1 (%)	11.0	3.8	8.4	5.2	5.3	3.8	2.0	1.6	5.0
	CalcM	49.8	49.8	49.8	49.8	49.8	49.8	49.8	49.8	
	Abs. Dev. 2 (%)	41.9	4.2	0.1	6.4	6.3	4.2	0.3	29.8	7.9
6	SlicingM	12.8	35.2	47.5	48.7	50.8	52.2	35.0	20.5	
	X-rayM	16.0	40.0	50.0	53.0	48.0	49.0	42.0	17.0	
	Abs. Dev. 1 (%)	25.0	13.6	5.3	8.9	5.5	6.0	20.0	16.9	12.4
	CalcM	13.4	37.4	49.9	52.3	51.9	48.0	29.9	13.4	
	Abs. Dev. 2 (%)	4.4	6.1	5.0	7.5	2.2	8.0	14.6	27.6	7.6
30	SlicingM	8.2	19.7	38.4	43.7	40.4	33.9	17.9	8.9	
	X-rayM	12.0	24.0	38.0	40.0	37.2	30.0	20.0	11.0	
	Abs. Dev. 1 (%)	47.2	22.1	1.0	8.4	7.8	11.4	11.8	23.9	12.9
	CalcM	8.2	23.1	38.1	43.6	42.6	34.0	18.2	8.2	
	Abs. Dev. 2 (%)	0.6	17.7	0.7	0.3	5.4	0.4	1.9	7.6	5.2
45	SlicingM	11.6	12.3	25.2	34.2	35.3	30.2	12.1	10.6	
	X-rayM	11.4	16.6	29.4	37.1	36.0	29.9	15.2	10.1	
	Abs. Dev. 1 (%)	1.2	35.3	16.4	8.7	2.1	1.1	25.4	4.1	11.8
	CalcM	8.2	16.9	26.5	36.1	33.3	22.8	14.0	8.2	
	Abs. Dev. 2 (%)	29.2	37.6	4.9	5.8	5.6	24.6	15.4	22.3	12.6
70	SlicingM	8.3	12.0	18.2	26.9	23.9	18.3	14.4	7.2	
	X-rayM	8.6	14.2	19.1	27.6	27.2	21.1	14.7	9.1	
	Abs. Dev. 1 (%)	3.9	17.9	4.7	2.3	13.9	15.6	1.8	26.8	11.0
	CalcM	8.0	14.0	20.1	27.0	24.9	17.9	11.9	8.0	
	Abs. Dev. 2 (%)	3.0	15.9	10.2	0.1	4.3	2.2	17.6	11.7	7.3
100	SlicingM	8.0	11.0	12.7	12.8	12.9	12.5	11.0	7.0	
	X-rayM	8.0	10.9	13.0	12.8	12.9	12.0	11.7	7.5	
	Abs. Dev. 1 (%)	0.6	0.8	2.1	0.5	0.2	3.5	6.4	6.6	2.6
	CalcM	7.9	11.1	12.9	14.1	13.9	12.4	10.1	7.9	
	Abs. Dev. 2 (%)	0.6	0.4	1.6	10.7	7.8	0.2	7.8	13.1	6.7
120	SlicingM	7.9	7.6	8.1	8.5	8.7	8.4	7.6	7.0	
	X-rayM	8.0	7.7	8.2	8.6	8.7	8.5	7.8	7.3	
	Abs. Dev. 1 (%)	0.9	1.1	1.6	1.3	0.7	1.6	2.5	4.4	1.8
	CalcM	7.8	8.0	8.5	9.1	9.0	8.3	7.9	7.8	
	Abs. Dev. 2 (%)	1.1	5.7	4.9	8.2	3.2	0.6	4.3	11.7	4.7

[a] SlicingM = ovendry-determined values; X-rayM = X-ray–determined values; CalcM = calculated curve; Abs. Dev. 1 = absolute deviations of moisture content comparing the slicing method and the X-ray radiation method; Abs. Dev. 2 = absolute deviations of moisture content comparing the slicing method and the calculated curve.

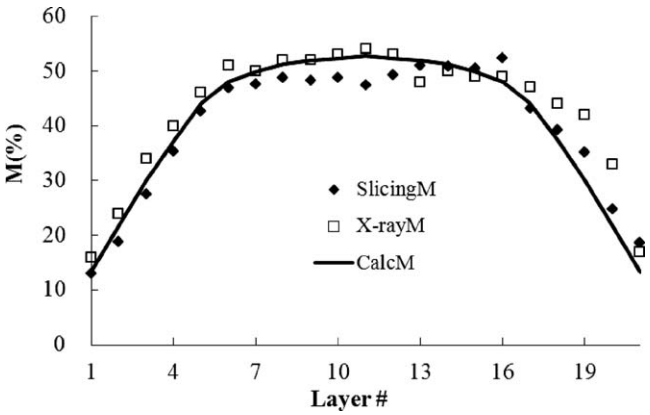

Figure 6.—Moisture content gradients after 6 hours of drying (Period 1). SlicingM = ovendry-determined values; X-rayM = X-ray–determined values; CalcM = calculated curve.

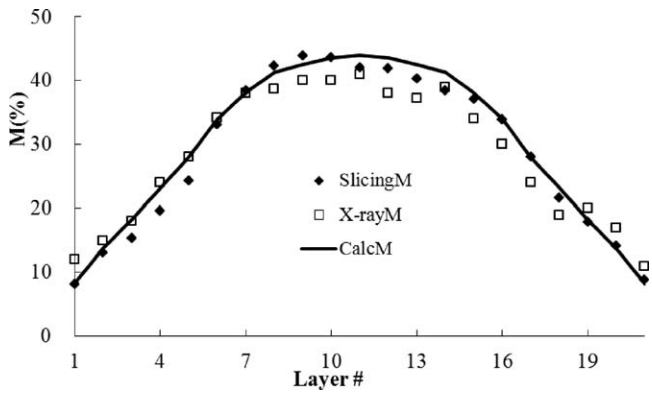

Figure 7.—Moisture content gradients after 30 hours of drying (Period 2). SlicingM = ovendry-determined values; X-rayM = X-ray–determined values; CalcM = calculated curve.

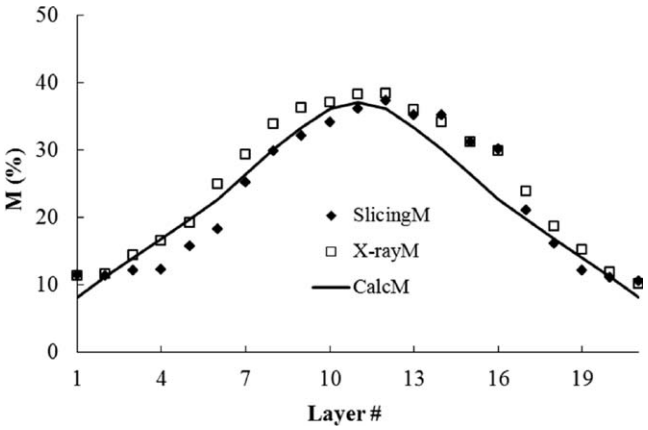

Figure 8.—Moisture content gradients after 45 hours of drying (Period 3). SlicingM = ovendry-determined values; X-rayM = X-ray–determined values; CalcM = calculated curve.

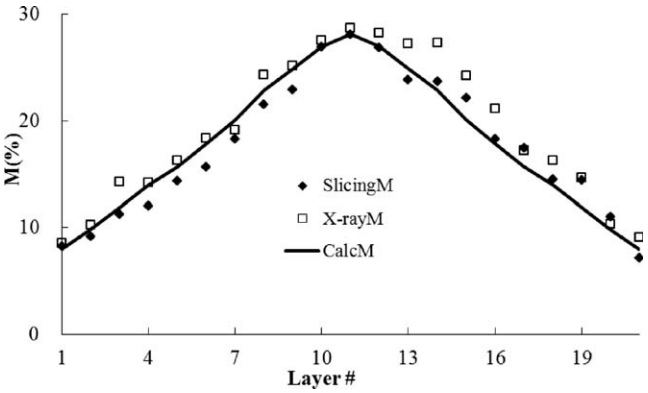

Figure 9.—Moisture content gradients after 70 hours of drying (Period 4). SlicingM = ovendry-determined values; X-rayM = X-ray–determined values; CalcM = calculated curve.

examinations. Abs. Dev. 1 in Table 1 is the comparison of MC between the slicing method and X-ray radiation. Compared with the MC values obtained by the ovendry slicing method, X-ray radiation is capable of determining MC to within ±12.9 percent. Abs. Dev. 2 in Table 1 is the comparison of MC between the slicing method and model estimation method. It shows that the model is capable of predicting MC values to within ±12.6 percent.

Figures 5 to 11 show that most calculated MC curves satisfactorily followed the MC values obtained by the ovendry slicing method. Table 1 also illustrates that the highest absolute deviations in Layers 1 and 21 between the slicing method and model-estimated values (Abs. Dev. 2) were 41.9 and 29.8 percent, respectively. The relatively greater errors in the surface layers were probably caused by the time required for slicing samples. When the specimens were taken out from the dryer and cut into samples that were further sliced into sections (Fig. 1), the surface layers of the samples were equilibrated with the room equilibrium MC, which was approximately 10 to 12 percent.

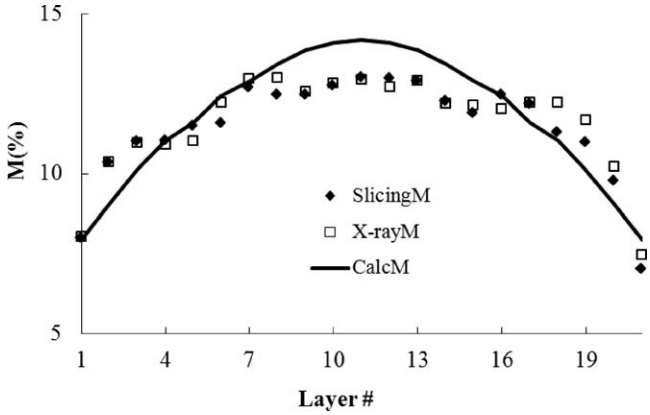

Figure 10.—Moisture content gradients after 100 hours of drying (Period 5). SlicingM = ovendry-determined values; X-rayM = X-ray–determined values; CalcM = calculated curve.

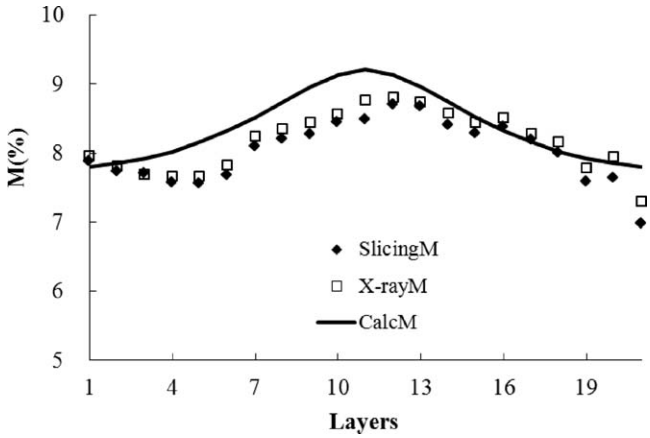

Figure 11.—Moisture content gradients after 120 hours of drying (Period 6). SlicingM = ovendry-determined values; X-rayM = X-ray–determined values; CalcM = calculated curve.

Conclusions

1. The results from the comparison of moisture gradients measured by the ovendry slicing method and X-ray radiation confirmed that the X-ray method can be used for monitoring moisture movement and distribution during the drying of Chinese fir to provide prompt information about internal stresses that could result in warping and defect development in lumber. Compared with the MC values obtained by the ovendry slicing method, the X-ray radiation method is capable of examining MC to within ±12.9 percent.
2. The results also indicated that the numeric model developed in this study can be used to estimate moisture gradients during the drying of Chinese fir. Compared with MC values measured by the ovendry slicing method, the model is capable of predicting moisture distribution to within ±12.6 percent.

Acknowledgment

This work was funded by the National Natural Science Foundation of China (No. 30825034).

Literature Cited

Alkan, S., Y. Zhang, and F. Lam. 2007. Moisture distribution changes and wetwood behavior in subalpine fir wood during drying using high X-ray energy industrial CT scanner. *Drying Technol*. 25(3):483–488.

Baettig, R., R. Remond, and P. Perre. 2006. Measuring moisture content profiles in a board during drying: A polychromatic X-ray system interfaced with a vacuum/pressure laboratory kiln. *Wood Sci. Technol*. 40(4):261–274.

Cai, L. 2005a. Determination of diffusion coefficients for sub-alpine fir. *Wood Sci. Technol*. 39(2):153–162.

Cai, L. 2005b. An estimation of heating rates in sub-alpine fir lumber. *Wood Fiber Sci*. 37(2):275–282.

Cai, Z. 2008. A new method of determining moisture gradient in wood. *Forest Prod. J*. 58(7/8):41–45.

Cai, L. and L. C. Oliveira. 2008. A simulation of wet pocket lumber drying. *Drying Technol*. 26(5):525–529.

Freyburger, C., F. Longuetaud, F. Mothe, T. Constant, and J. M. Leban. 2009. Measuring wood density by means of X-ray computer tomography. *Ann. Forest Sci*. 66(9):804–813.

Haquea, N. 2007. Simulation of temperature and moisture content profiles in a *Pinus radiata* board during high-temperature drying. *Drying Technol*. 25(4):547–555.

Hattori, Y. and Y. Kanagawa. 1985. Nondestructive measurement of moisture distribution in wood with a medical X-ray CT scanner. I. Accuracy and influencing factor. *J. Jpn. Wood Res. Soc*. 31(12):974–982.

Kanagawa, Y. and Y. Hattori. 1985. Nondestructive measurement of moisture distribution in wood with a medical X-ray CT scanner. II. Changes in moisture distribution with drying. *J. Jpn. Wood Res. Soc*. 31(2):983–989.

Koumoutsakos, A. and S. Avramidis. 2002. Mass transfer characteristics of western hemlock and western red cedar. *Holzforschung* 56(2):185–190.

Kreith, F. and M. S. Bohn. 2001. Heat conduction, chap. 2. *In:* Principles of Heat Transfer. 6th ed. Brooks/Cole Thomson Learning, Pacific Grove, California. pp. 184–196.

Lindgren, L. O. 1991. Medical CAT-scanning: X-ray absorption coefficients, CT-numbers and their relation to wood density. *Wood Sci. Technol*. 25(5):341–349.

Lindgren, O., J. Davis, P. Wells, and P. Shadbolt. 1992. Non-destructive wood density distribution measurements using computed tomography. *Eur. J. Wood Wood Prod*. 50(7–8):295–299.

Liu, J. Y., W. T. Simpson, and S. P. Verrill. 2001. An inverse moisture diffusion algorithm for the determination of diffusion coefficient. *Drying Technol*. 19(8):1555–1568.

Pang, S. 2007. Mathematical modeling of kiln drying of softwood timber: Model development, validation, and practical application. *Drying Technol*. 25(3):421–431.

Pang, S. and P. Wiberg. 1998. Model predicted and CT scanned moisture distribution in a *Pinus radiata* board during drying. *Eur. J. Wood Wood Prod*. 56(1):9–14.

Pordage, L. J. and T. A. G. Langrish. 1999. Simulation of the effect of air velocity in the drying of hardwood timber. *Drying Technol*. 17(1–2):237–255.

Watanabea, K., Y. Saitoa, S. Avramidis, and S. Shida. 2008. Non-destructive measurement of moisture distribution in wood during drying using digital x-ray microscopy. *Drying Technol*. 26(5):590–595.

Zhang, Y. and L. Cai. 2011. Modeling and microscopic analysis of vaporization during high temperature drying of sub-alpine fir. *Drying Technol*. 29(10):1179–1185.